

Review Article

Black Titanium Dioxide Nanomaterials in Photocatalysis

Xiaodong Yan, Yong Li, and Ting Xia

Department of Chemistry, University of Missouri-Kansas City, Kansas City, MO 64110, USA

Correspondence should be addressed to Yong Li; liyong@umkc.edu

Received 30 June 2017; Accepted 11 September 2017; Published 2 November 2017

Academic Editor: P. Davide Cozzoli

Copyright © 2017 Xiaodong Yan et al. This is an open access article distributed under the Creative Commons Attribution License, which permits unrestricted use, distribution, and reproduction in any medium, provided the original work is properly cited.

Titanium dioxide (TiO_2) nanomaterials are widely considered to be state-of-the-art photocatalysts for environmental protection and energy conversion. However, the low photocatalytic efficiency caused by large bandgap and rapid recombination of photo-excited electrons and holes is a challenging issue that needs to be settled for their practical applications. Structure engineering has been demonstrated to be a highly promising approach to engineer the optical and electronic properties of the existing materials or even endow them with unexpected properties. Surface structure engineering has witnessed the breakthrough in increasing the photocatalytic efficiency of TiO_2 nanomaterials by creating a defect-rich or amorphous surface layer with black color and extension of optical absorption to the whole visible spectrum, along with markedly enhanced photocatalytic activities. In this review, the recent progress in the development of black TiO_2 nanomaterials is reviewed to gain a better understanding of the structure-property relationship with the consideration of preparation methods and to project new insights into the future development of black TiO_2 nanomaterials in photocatalytic applications.

1. Introduction

Titanium dioxide (TiO_2) nanomaterials have been considered as the most promising semiconductor photocatalysts for pollutant removal and energy generation owing to their relatively good photocatalytic activity, low cost, nontoxicity, and high stability since the discovery of hydrogen evolution through the photoelectrochemical water splitting on TiO_2 electrode [1–3]. Meanwhile, photocatalysis potentially can be an ideal solution to current environmental issues and energy crisis by only consuming solar energy. Over the past decades, nanotechnology has greatly contributed to the development of TiO_2 materials in photocatalysis across the globe [2–7]. However, the large bandgaps (3.0–3.2 eV over different phases) of TiO_2 nanomaterials limit their optical absorption to ultraviolet (UV) light, along with the rapid recombination of photo-excited electrons and holes, resulting in low photocatalytic efficiency [1–11]. Extending the utilization of solar energy to visible region has thus been the urgent need for practical applications of TiO_2 nanomaterials.

The optical and electronic properties of solid materials highly depend on the structure including the way the atoms are bonded and arranged, the phases and their distribution,

and the defects [12–16]. Therefore, tuning these states in solid materials can potentially tailor the optical and electronic properties of the existing solid materials [17–19]. Since the discovery of visible-light active nitrogen-doped TiO_2 [19], structural modification of TiO_2 nanomaterials has been at the research frontier to extend the utilization of solar light to visible region, while other methods, such as localized surface plasmon resonance of plasmonic nanostructures [18, 20, 21], have been exploited. In 2011, the electronic band structure of black TiO_2 nanocrystals was reported to be largely narrowed for massive visible light absorption and conversion to chemical energy, leading to markedly enhanced photocatalytic activity towards photocatalytic pollution removal and hydrogen generation from water [22]. Since then black TiO_2 nanomaterials have attracted unprecedented interest in visible light utilization. Over the past decade, many methods, such as hydrogenation, aluminum reduction, and chemical reduction, have been developed to synthesize black TiO_2 nanomaterials. In this review, we focus on the recent research progress in black TiO_2 nanomaterials for photocatalytic applications, especially for photocatalytic hydrogen generation and pollutant removal. The basic properties of black TiO_2 nanomaterials

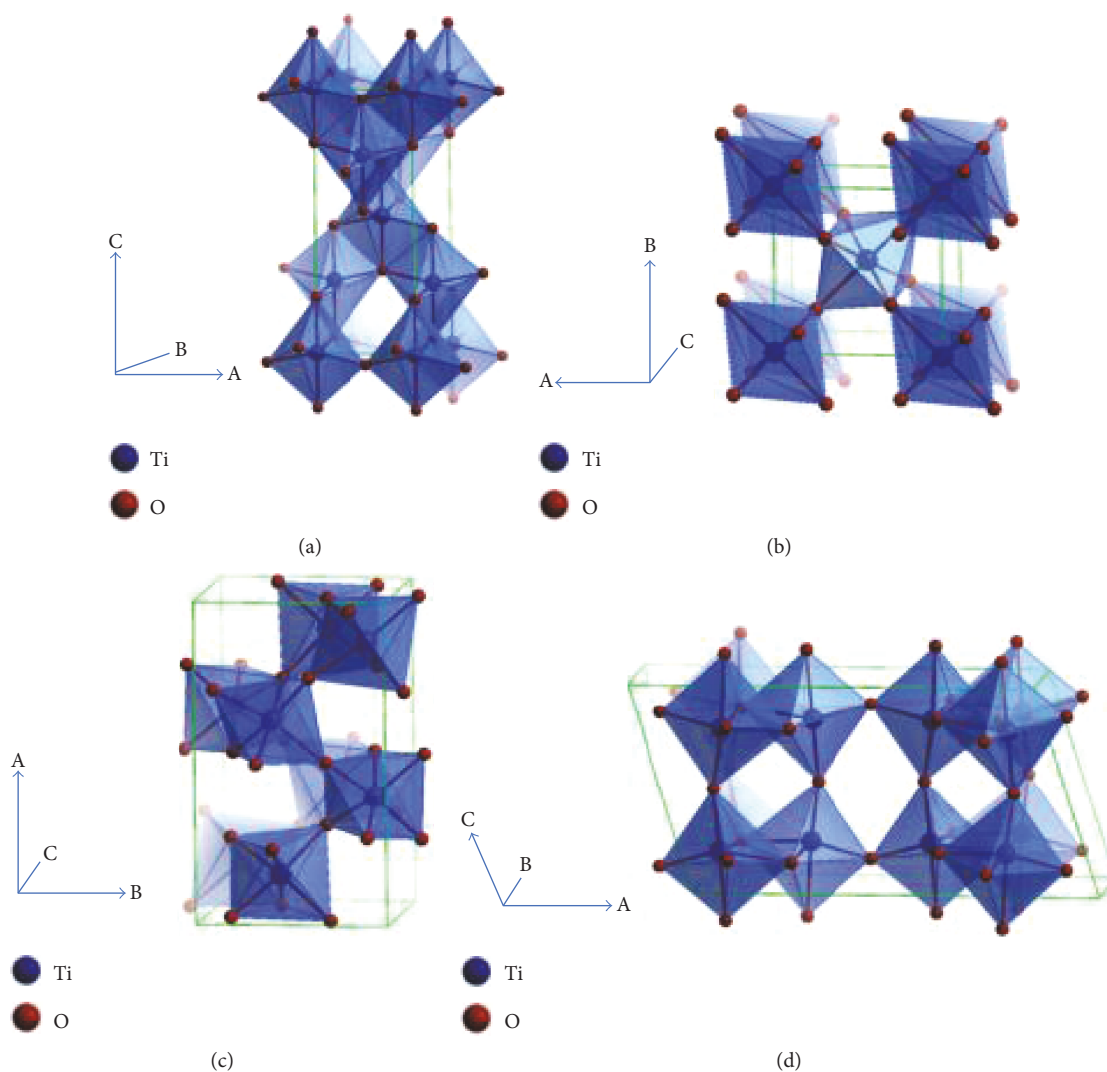


FIGURE 1: Crystalline structures of TiO₂ in different phases: (a) anatase, (b) rutile, (c) brookite, and (d) TiO₂(B). Reprinted with permission from [25]. Copyright (2014) American Chemical Society.

are first discussed in brief, and then, typical examples are given for each preparation method. We aim to get a better understanding on the relationship between the structure and photocatalytic properties of black TiO₂ nanomaterials from different preparation methods, along with considering the effect of preparation methods on their structures. Finally, summary and perspectives on the development of black TiO₂ nanomaterials are addressed.

2. Basic Properties of Black TiO₂ Versus White TiO₂

TiO₂ exists in different phases. Anatase, rutile, brookite, and TiO₂(B) are the four main polymorphs of TiO₂. It is widely acknowledged that rutile is thermodynamically the most stable phase, while anatase, brookite, and TiO₂(B) are metastable phases. The metastable phases of TiO₂ will go through phase transformation at elevated temperatures. Usually, it is considered that anatase goes through phase transformation to rutile [23, 24] and brookite and TiO₂(B) to anatase then

to rutile [25, 26]. However, exceptions have been reported. Direct transformation of brookite to rutile is observed, while in the case of the anatase–brookite mixture, anatase transforms firstly to brookite and then to rutile [27]. It is suggested that the phase transformation process is affected by various parameters.

Generally, anatase and rutile TiO₂ nanomaterials can be easily prepared using conventional preparation methods, while the preparation of brookite and TiO₂(B) nanomaterials needs special attention. Anatase is relatively stable, and the phase transformation between anatase and rutile is dependent on a variety of factors, such as particle size and defects in anatase TiO₂ [28, 29]. So far, anatase and rutile TiO₂ nanomaterials are the most widely studied photocatalysts.

Different phases have different structures. Generally, all four types of polymorphs mentioned above comprise of TiO₆ octahedra, but differ in the distortion of the octahedron units and share edges and corners in different manners (Figure 1) [25]. The differences in TiO₆ octahedra arrangement result in different physicochemical properties and thus

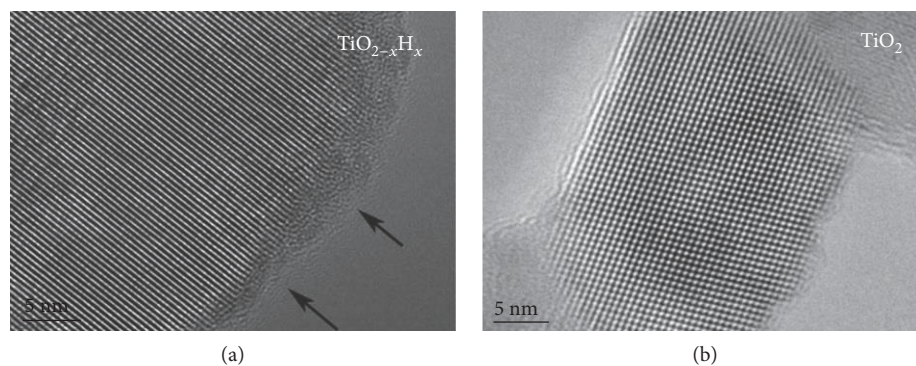


FIGURE 2: HRTEM images of (a) black hydrogenated TiO_2 ($\text{TiO}_{2-x}\text{H}_x$) and (b) white TiO_2 . Reprinted with permission from [33]. Copyright (2013) Wiley-VCH.

different photocatalytic activities. To the best of our knowledge, black TiO_2 nanomaterials have been prepared from white anatase, rutile, brookite, and $\text{TiO}_2(\text{B})$. It should be noted that phase transformation was observed in a very few cases when white TiO_2 nanomaterials converted into black ones during the modification process [23].

2.1. Basic Structure. Color change from white to black for TiO_2 nanomaterials reflects the change in optical properties and thus suggests the structural change after modification, at least the surface structural change. High-resolution transmission electron microscope (HRTEM) has revealed that a number of black TiO_2 nanomaterials have a crystalline/amorphous core/shell structure, while white ones have clear lattice fringes throughout the crystals [22, 23, 30–44]. The amorphous or disordered surface layer has been considered the typical feature of black TiO_2 nanomaterials. Figure 2 shows the HRTEM images of black and white TiO_2 nanomaterials with Figure 2(a) showing the typical core/shell structure of the black TiO_2 [33]. The combination of X-ray diffraction (XRD) and Raman measurements has also confirmed the surface structural differences between black and white TiO_2 nanomaterials. However, it should be noted that not all black TiO_2 nanomaterials have the crystalline/disordered core/shell structure.

2.2. Surface Functional Group. Surface $-\text{OH}$ groups exist in many TiO_2 nanomaterials depending on the preparation method. As hydrogen is used in hydrogen thermal treatment and hydrogen plasma treatment, it is very possible to generate $-\text{OH}$ groups on the surface of hydrogenated black TiO_2 nanomaterials owing to the reduction effect of hydrogen. An increase in $-\text{OH}$ groups has been detected in hydrogenated black TiO_2 nanomaterials by X-ray photoelectron spectroscopy (XPS) [22, 45]. Fourier transform infrared (FTIR) spectroscopy is another important technique to reveal the change in surface $-\text{OH}$ groups by comparing the magnitude of the intensity of the peak corresponding to the $-\text{OH}$ vibrational band [33, 34, 46]. In addition, ^1H nuclear magnetic resonance (NMR) technique has also been used to analyze the surface $-\text{OH}$ groups [33, 34].

The existence of $-\text{H}$ groups on the surface of black TiO_2 nanomaterials is very debatable. They have only been detected in a few cases of hydrogenated TiO_2 nanomaterials [33, 47]. Wang et al. attributed the peak at 457.1 eV in the Ti 2p XPS spectrum of the hydrogenated black TiO_2 nanocrystals to surface Ti–H bonds [33]. Zheng et al. found that hydrogenated TiO_2 nanowire microspheres exhibited one shoulder peak at the lower binding energy side of the broader Ti 2p peak in the XPS spectrum and attributed it to the surface Ti–H bonds formed under hydrogen atmosphere [47]. Formation of surface Ti–H bonds was at the expense of surface Ti–OH groups [47]. Such groups do not exist on the surface of white TiO_2 nanomaterials undoubtedly.

2.3. Defects. Oxygen vacancy is one of the most common defects existing in metal oxides including TiO_2 nanomaterials [48–50]. It has considerable influence on the activity and kinetics of the reactions proceeding on the surface of metal oxides [15, 48–51]. Oxygen vacancies are undetectable in most white TiO_2 nanomaterials, while oxygen vacancy is considered to be one of the feature defects in most black TiO_2 nanomaterials. Electron paramagnetic resonance (EPR) or electron spin resonance (ESR) spectroscopy [37–40, 52], Raman spectroscopy [9, 16, 32, 53–55], and X-ray diffractometer [23, 32, 55] have been used to detect the oxygen vacancies present in black TiO_2 nanomaterials.

Ti^{3+} defects do not exist in white TiO_2 as all Ti ions usually present in the form of Ti^{4+} . The presence of Ti^{3+} defects in black TiO_2 nanomaterials is debatable. Based on XPS technique, some researchers reported the absence of Ti^{3+} defects in black TiO_2 nanomaterials [22, 23, 34, 45, 46], while others argued the presence of Ti^{3+} defects derived from the reduction of Ti^{4+} ions [9, 16, 30, 53, 55–58]. More commonly, Ti^{3+} defects in black TiO_2 could be detected by EPR or ESR spectroscopy [30, 33, 37, 41, 52, 55, 57, 59, 60].

Oxygen vacancies and/or Ti^{3+} impurities are believed to be highly related to the color change of the defect-rich TiO_2 [14, 61–66]. More importantly, oxygen vacancies and/or Ti^{3+} defects extend the photoresponse of TiO_2 from UV to visible light region, which leads to high visible-light photocatalytic activity [14, 59, 67–72]. Note that high density of crystal defects, especially bulk defects, may accelerate electron-hole recombination as defects can

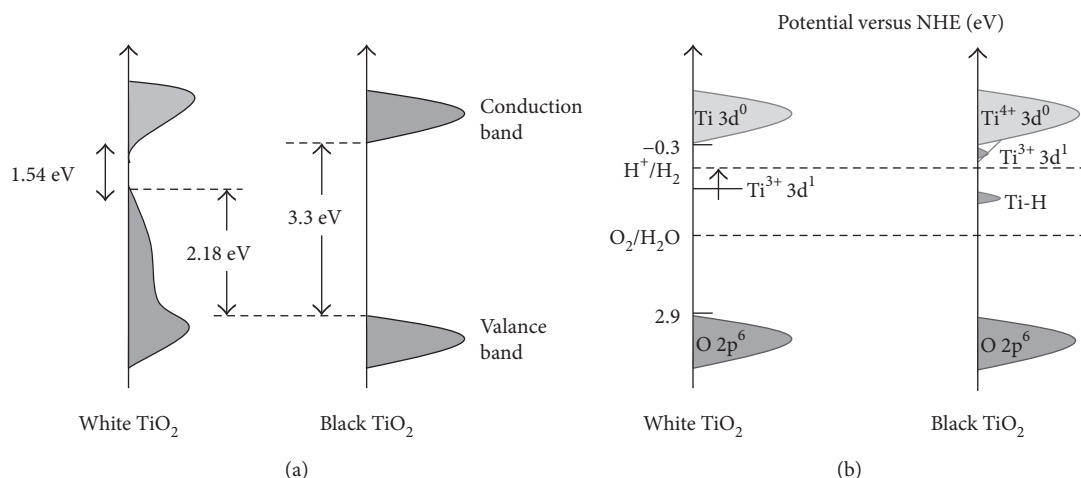


FIGURE 3: (a) Schematic illustration of the DOS of black and white TiO₂ nanocrystals. Reprinted with permission from [22]. Copyright (2011) American Association for the Advancement of Science. (b) Schematic illustration of the DOS of TiO₂ (Degussa P25) and black TiO₂ nanocrystals. Reprinted with permission from [33]. Copyright (2013) Wiley-VCH.

act as charge annihilation centers [57, 73, 74]. It is likely that surface oxygen vacancies are responsible for the enhanced photocatalytic activity [39, 70, 75], while bulk oxygen vacancies act as trap states and charge carrier recombination centers [76]. Studies also showed that surface Ti³⁺ defects could enhance hole trapping and thus facilitate the separation of photo-excited electrons and holes [57], while bulk Ti³⁺ sites acted as charge annihilation centers, leading to enhanced nonradiative recombination and shorter lifetime of electrons and holes [57, 60]. In addition, Ti³⁺ ions with oxygen vacancies can improve the electrical conductivity of TiO₂ [73, 77], which may enhance the charge transport and charge-transfer reaction [73].

2.4. Electronic Band Structure. The introduction of defects and/or surface disorder could result in change in electronic and optical properties of black TiO₂. Bandgap narrowing is a vivid demonstration of the change in band structure of black TiO₂. The origin of the bandgap narrowing has been argued for years owing to the complexity of the surface defects/disorders and functional groups. One assumption is that Ti³⁺ species in the bulk TiO₂ is responsible for the bandgap narrowing [14, 59, 67, 68], and the oxygen-vacancy mid-gap states further enhance the light absorption for photon energy below the direct bandgap by indirect electron transitions [14]. Chen et al. thought that bandgap narrowing mainly originated from the disorder-induced midgap states rather than the Ti³⁺ species, greatly upshifting the valence band (VB) edge of black TiO₂, and that the possible conduction band (CB) tail states arising from the surface disorder could only slightly narrow the bandgap (Figure 3(a)) [22, 34]. Naldoni's group agreed with these analyses and further pointed out that oxygen vacancies could introduce localized states at 0.7–1.0 eV below the CB minimum of black TiO₂ [23]. As shown in the schematic illustration of the density of states (DOS) of black and white TiO₂ (Figure 3(b)), Wang et al. reported that the CB and VB tails slightly narrowed the bandgap by 0.8 eV and that the Ti–H

bonds introduced the midgap electronic states at 0.92–1.37 eV below the CB minimum of black TiO₂ [33]. In summary, the change in band structure is mainly attributed to the tailing of VB and/or CB, and the midgap states are induced by oxygen vacancies or –H groups [22, 23, 33, 39].

3. Fundamental Physicochemical Process in Photocatalysis

A simplified model representing the fundamental physicochemical process in photocatalysis is demonstrated in Figure 4. A typical process of photocatalysis involves three steps: light absorption, electron-hole separation, and surface reaction. Light with energy greater than the bandgap of TiO₂ nanocrystal excites an electron from the VB to the CB; meanwhile, a positive hole will be left in the VB. In the case of anatase TiO₂ with a bandgap of 3.2 eV, UV light with $\lambda \leq 387$ nm is required for electron excitation. The electrons and holes that have been separated and transferred onto the surface of TiO₂ can trigger redox reactions (pathways 1 and 2). For example, the electrons scavenged by O₂ can yield superoxide radical anions, while the holes that react with H₂O can produce hydroxyl radicals. These radicals can oxidize organic species, such as methylene blue [6], rhodamine B and salicylic acid [8], and methylene orange [9]. Thus, photocatalysis can be applied in degradation of pollutants [6, 8, 9], reduction of CO₂ [10], and water splitting [1, 6]. However, electrons and holes may recombine on the surface (surface recombination, namely, pathway 3) or even in the bulk (volume recombination, namely, pathway 4) [74], which will compete with the desired redox reactions and thus greatly decrease the efficiency of the photocatalytic process. To increase the utilization of solar energy, the bandgap of TiO₂ needs to be engineered to extend its optical absorption from UV to visible even to infrared light. On the other hand, the charge carrier separation must be exponentially enhanced in order to improve the photocatalytic efficiency and achieve the ultimate practical applications of TiO₂ in photocatalysis.

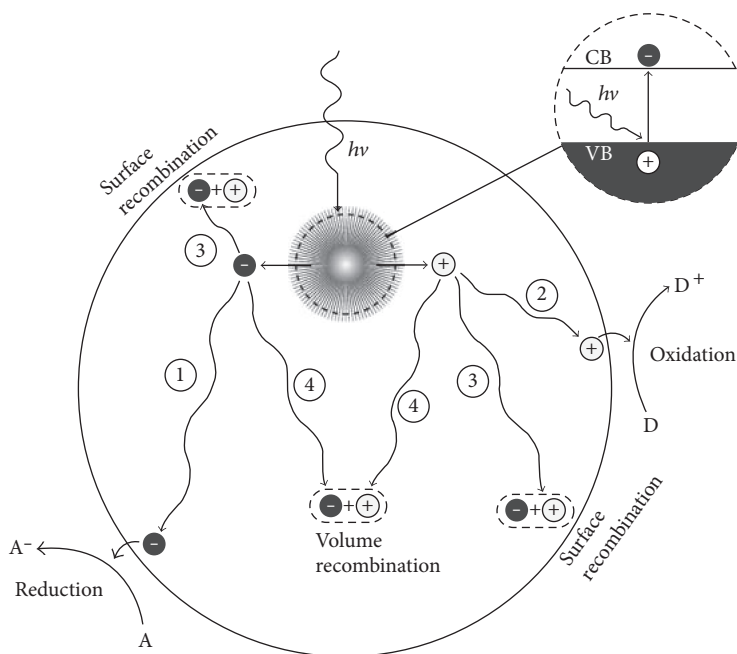


FIGURE 4: Schematic demonstration of the photocatalytic mechanism of TiO_2 . A is electron acceptor, and D is electron donor. Reprinted with permission from [10]. Copyright (2013) Wiley-VCH.

4. Black TiO_2 Nanomaterials as Visible Light-Active Photocatalysts

Black TiO_2 nanomaterials have been synthesized by various methods including hydrogen thermal treatment, hydrogen plasma treatment, chemical reduction, chemical oxidation, and electrochemical reduction. Although those black TiO_2 nanomaterials have similar appearance, their microstructures may differ owing to the differences in preparation methods and reaction parameters, and thus, black TiO_2 nanomaterials from different research groups worldwide possess different physicochemical properties. Herein, we will give a few typical examples for each preparation method.

4.1. Black TiO_2 Nanomaterials by Hydrogenation. Since the discovery of black TiO_2 by Chen et al. in 2011 [22], hydrogenation or hydrogen reduction has become a powerful tool to synthesize black TiO_2 nanomaterials. A variety of parameters, such as source of raw TiO_2 , hydrogenation time and temperature, H_2 pressure, exposed crystal facet of TiO_2 , and even reactor materials, will affect the colorization, surface structure and groups, and photocatalytic performance of hydrogenated TiO_2 nanomaterials [22, 23, 36, 40, 45–47, 52, 73, 76–80]. Note that the crystalline/disordered core/shell structure is only observed in a few hydrogenated black TiO_2 nanomaterials [22, 23, 36, 78]. Chen et al. synthesized black TiO_2 nanocrystals by high-pressure hydrogenation in a 20.0-bar H_2 atmosphere at about 200°C for 5 days [22]. The raw TiO_2 nanocrystals were prepared with a precursor solution consisting of titanium tetraisopropoxide, ethanol, hydrochloric acid, deionized water, and Pluronic F127 as an organic template, followed by hydrolysis at 40°C for 24 h, solvent evaporation at 110°C for 24 h, and calcination at 500°C

for 6 h in air [22]. The disorder-engineered black TiO_2 nanomaterials contain two phases with a core/shell structure: a crystalline core and a disordered or amorphous shell (Figure 5). The crystalline phase of the black TiO_2 maintained the anatase structure of the white raw TiO_2 as evidenced by XRD analysis, whereas peak broadening and extra peaks besides the typical signals of anatase TiO_2 were observed in the Raman spectrum of the black TiO_2 owing to the disordered nature of the surface layer [22]. When used as photocatalysts, the degradation rate of methylene blue on the black TiO_2 nanocrystals was found to be nearly 7 times that on the raw TiO_2 nanocrystals, and the photocatalytic H_2 production rate of the black TiO_2 using 1:1 water-methanol solution under sunlight reached as high as $10 \text{ mmol}\cdot\text{h}^{-1}\cdot\text{g}^{-1}$ [22]. The high photocatalytic activity was ascribed to the substantially narrowed bandgap (experimentally $\sim 1.54 \text{ eV}$) induced by the surface disorder, thus extending the optical absorption from UV to infrared region [22]. First-principle density functional theory calculation showed that two midgap states (centered at ~ 1.8 and $\sim 3.0 \text{ eV}$ corresponding to the VB and CB band tails, resp.) were created in the black TiO_2 nanocrystals and thus well explained the origin of the change in the electronic and optical properties of black TiO_2 nanocrystals [22].

Black rutile TiO_2 nanowires have been prepared by hydrogenation in a tube furnace filled with ultrahigh purity hydrogen gas at temperatures $\geq 450^\circ\text{C}$ for 30 min for photoelectrochemical water splitting [45]. Pristine rutile TiO_2 nanowires were grown on a fluorine-doped tin oxide (FTO) glass substrate by hydrothermal method with titanium n-butoxide in aqueous hydrochloric acid solution at 150°C for 5 h, followed by annealing in air at 550°C for 3 h to increase the crystallinity of TiO_2 nanowires and improve their contact

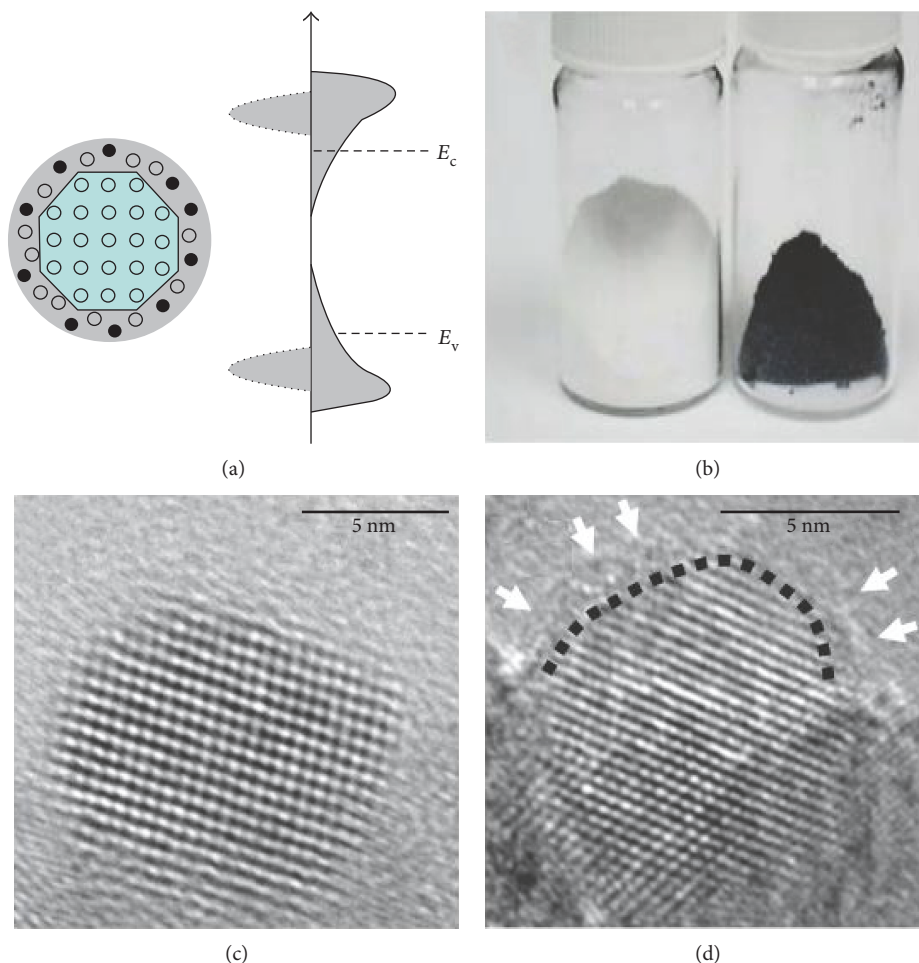


FIGURE 5: (a) Schematic illustration of the structure and electronic DOS of a disorder-engineered semiconductor nanocrystal with dopant incorporation. Dopants are depicted as black dots, and disorder is represented in the outer layer of the nanocrystal. E_C and E_V represent the conduction and valence levels of a bulk semiconductor, respectively. The intrinsic bands of the nanocrystal are shown at the left. The disorder-induced CB and VB tails extending into the otherwise forbidden levels are shown at the right. (b) Digital images of the white and black TiO_2 nanocrystals. (c and d) HRTEM images of the white and black TiO_2 nanocrystals. Reprinted with permission from [22]. Copyright (2011) American Association for the Advancement of Science.

to the substrate [45]. In this study, the authors found that the enhanced photoactivity of the black TiO_2 nanowires was mainly attributed to the facilitated charge transport in black TiO_2 and charge separation at the TiO_2 /electrolyte interface owing to the increased donor density or oxygen vacancies, while the visible light absorption only made a negligible contribution [45]. Further study showed that the electronic band structure of the black TiO_2 nanowires was similar to that of the pristine TiO_2 nanowires, and the color change was owed to the impurity/defect states in the bandgap of the black TiO_2 nanowires caused by oxygen vacancies [45]. Similar enhancement in photoactivity of the hydrogenated anatase TiO_2 nanotubes was observed in this study [45].

Liu et al. fabricated black anatase TiO_2 nanotubes by anodic oxidation and hydrogenation [52]. In a typical synthesis, clean titanium foils were anodized in a two-electrode configuration with platinum gauze as the counter electrode in the electrolyte containing ethylene glycol (less than 0.2 wt.% H_2O), deionized water (1 M), and NH_4F (0.1 M) at

60 V for 15 min; black TiO_2 nanotubes were then achieved by atmospheric pressure hydrogenation in H_2/Ar (5%) flow at 500°C for 1 h [52]. The authors compared the effect of a series of factors on the photoactivity of the hydrogenated TiO_2 . It was found that atmospheric pressure (H_2/Ar) hydrogenated anatase TiO_2 nanotubes had more oxygen vacancies, while high-pressure (20.0 bar, 500°C for 1 h) hydrogenated anatase TiO_2 nanotubes possessed more Ti^{3+} species [52]. Photocatalytic experiments demonstrated that high-pressure hydrogenated anatase TiO_2 nanotubes exhibited a high H_2 evolution rate of $7 \mu\text{mol}\cdot\text{h}^{-1}\text{cm}^{-2}$ without any cocatalysts, while atmospheric pressure hydrogenated anatase TiO_2 nanotubes had negligible H_2 evolution [52]. For reference, rutile nanorods hydrogenated in either atmospheric pressure or high-pressure hydrogen showed extremely small H_2 evolution rate [52]. It is believed that different polymorphs using anatase and rutile as examples have different defect formation behaviors upon reductive treatments [66, 81, 82] and thus lead to different photoactivities of treated TiO_2 nanomaterials.

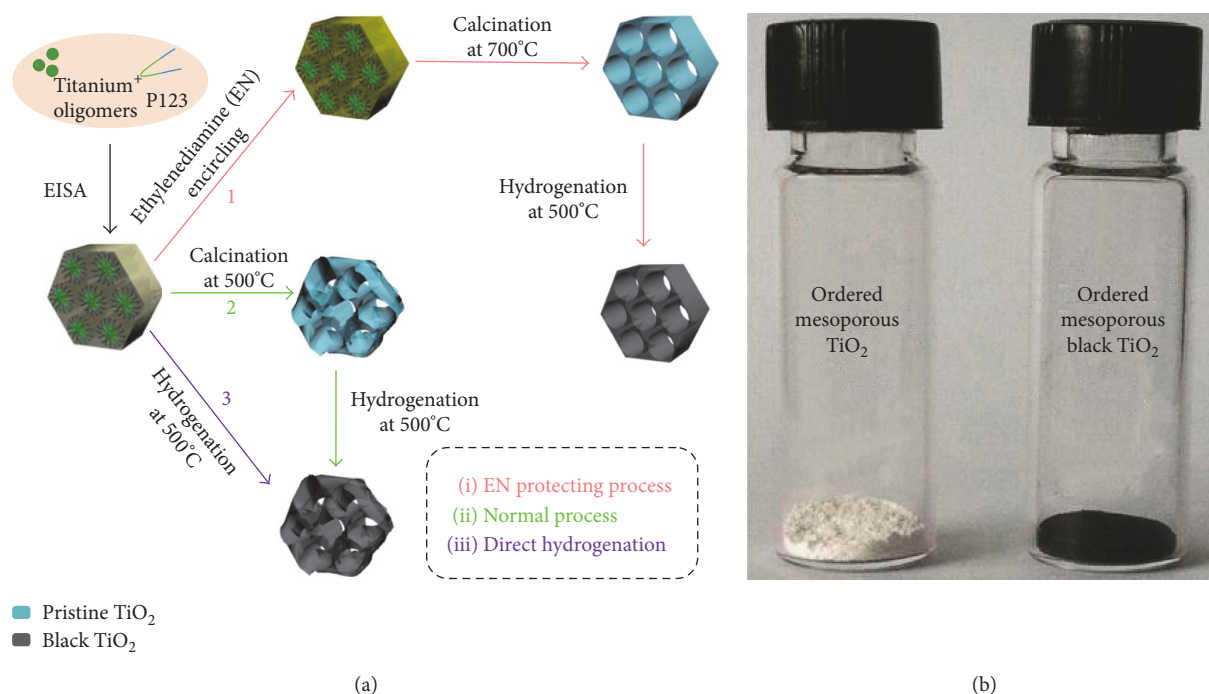


FIGURE 6: (a) Schematic synthesis process for the ordered mesoporous black TiO₂ materials and (b) the ordered mesoporous TiO₂ before and after hydrogenation. Reprinted with permission from [78]. Copyright (2014) American Chemical Society.

Recently, ordered mesoporous black anatase TiO₂ was prepared through an evaporation-induced self-assembly method combined with an ethylenediamine encircling process, followed by atmospheric pressure hydrogenation at 500°C for 3 h under H₂ flow [78]. Figure 6(a) displays the schematic synthesis process. Interestingly, the ordered mesoporous TiO₂ prepared with ethylenediamine turned into a black color after hydrogenation (Figure 6(b)), whereas only gray TiO₂ was obtained with the porous TiO₂ synthesized without ethylenediamine [78]. This suggested that the original surface functionalities and surface structural defects may be the very important factors determining the colorization or types of defects or electronic band structure of the hydrogenated TiO₂ nanomaterials. The VB XPS analysis found that the VB maximum energy for the black TiO₂ blue-shifted towards the vacuum level at ~1.6 eV owing to the possible Ti³⁺ species, narrowing the bandgap to ~2.80 eV consistent with the experimental value of 2.82 eV [78]. The resultant ordered mesoporous black TiO₂ showed an extended photoresponse from UV light to visible and infrared light regions and thus exhibited a high photocatalytic hydrogen evolution rate of 136.2 μmol·h⁻¹, which approached two times that (76.6 μmol·h⁻¹) of the pristine ordered mesoporous TiO₂ [78].

4.2. Black TiO₂ Nanomaterials by Hydrogen Plasma. Hydrogen plasma technology has attracted increasing interest owing to its effectiveness in engineering surface-disordered TiO₂ nanomaterials with a typical crystalline/amorphous core/shell structure [33, 39, 57, 60]. Ti³⁺ species and oxygen vacancies were reported to be the primary defects in some cases [57, 58], while Ti-H groups and oxygen vacancies were believed to be the dominant defects in other cases [33, 39].

H-doped black titania (TiO_{2-x}H_x) with high solar absorption (~83%) was converted from commercial TiO₂ (Degussa P25) in a thermal plasma furnace by hydrogen plasma for 4–8 h at 500°C with the plasma input power of 200 W [33]. The TiO_{2-x}H_x presented a crystalline/amorphous core/shell structure, and the black coloration of TiO_{2-x}H_x was possibly caused by the defects including H doping, oxygen vacancies and surface hydroxyl groups [33]. As discussed above in Section 2.4, the tailing effect of VB and CB and the midgap states caused by H doping contributed to the Vis-NIR absorption of the black TiO_{2-x}H_x and thus highly enhanced photocatalytic activity [33]. The TiO_{2-x}H_x showed much higher solar-to-electron efficiency in both photocatalytic water splitting (Figure 7(a)) and degradation of methyl orange over pristine TiO₂ (Figure 7(b)) and demonstrated a high cycling stability (Figure 7(c)) [33].

Black TiO₂ nanocrystals with the typical crystalline/amorphous core/shell structure were prepared from hydrogen plasma treatment of commercial TiO₂ nanoparticles (Degussa P25) by Yan et al. [57]. Surprisingly, the authors found that slightly hydrogenated TiO₂ nanocrystals without visible coloration exhibited enhanced photoactivity in both photocatalytic degradations of methylene blue and reduction of CO₂ with H₂O, while gray and black TiO₂ showed worse photoactivity over pristine TiO₂ [57]. It was proposed that improved photocatalytic performance of slightly hydrogenated TiO₂ could be attributed to the higher ratio of trapped holes (O⁻ centers) and a lower recombination rate induced by the increase of surface defects, while the highly concentrated bulk defects in gray and black (overhydrogenated) TiO₂ acted as charge recombination centers, leading to worse photoactivity [57].

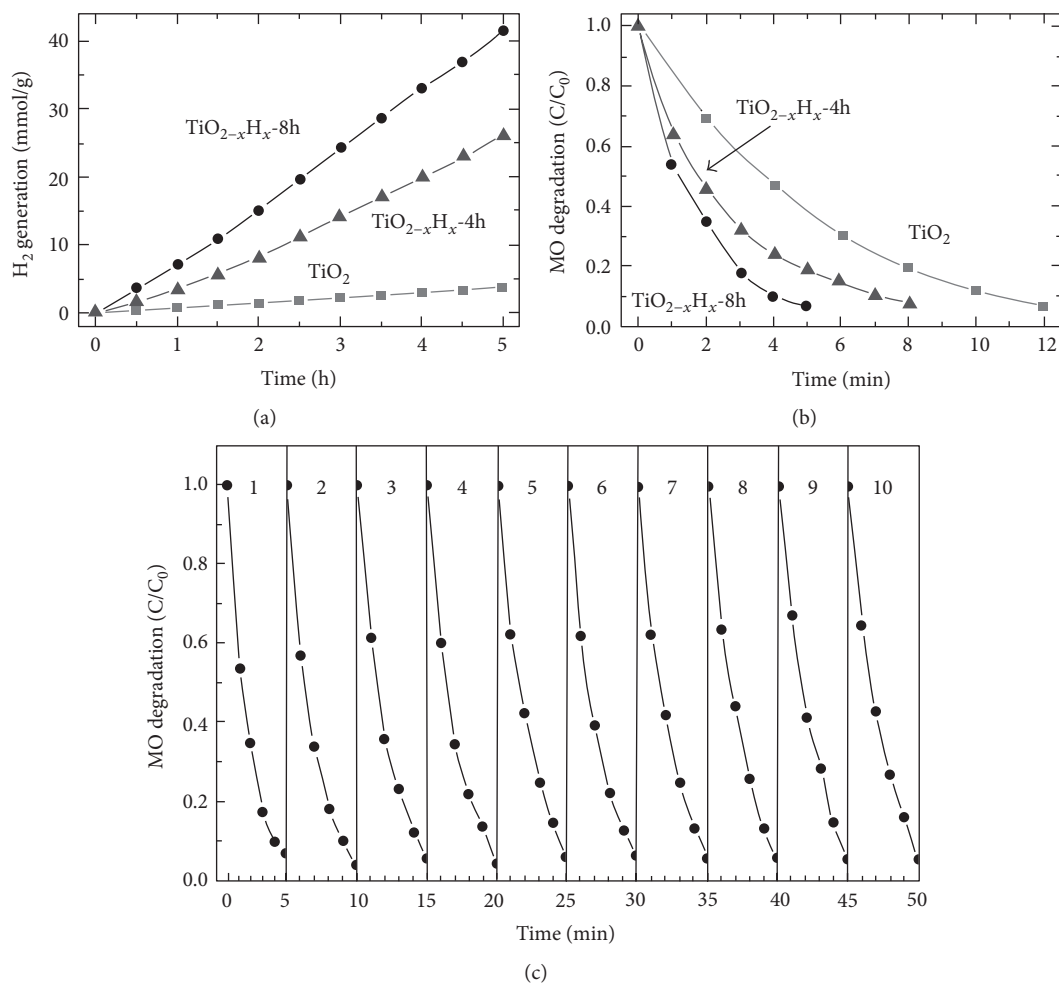


FIGURE 7: Solar light-driven photocatalytic (a) water splitting for H₂ generation and (b) decomposition of methyl orange over pristine TiO₂, TiO_{2-x}H_x-4h, and TiO_{2-x}H_x-8h. (c) Cycling tests of solar-driven photocatalytic activity of TiO_{2-x}H_x-8h. Reprinted with permission from [33]. Copyright (2013) Wiley-VCH.

4.3. Black TiO₂ Nanomaterials by Chemical Reduction

4.3.1. Aluminum Reduction. Huang's group has reported on the synthesis of a series of black TiO₂ nanomaterials by aluminum reduction [9, 32, 37, 38, 41, 53]. The typical crystalline/amorphous core/shell structure was observed in almost all Al-reduced black TiO₂ [9, 32, 37, 38, 41], except for the black TiO₂ nanotubes [53]. Also, Ti³⁺ and oxygen vacancy defects were commonly detected in Al-reduced black TiO₂ [9, 32, 37, 38, 41, 53]. In a typical synthesis of the Al-reduced black TiO₂, aluminum and pristine TiO₂ (Degussa P25) were placed separately in a two-zone tube furnace (Figure 8(a)); the pressure in the tube was controlled at a base pressure below 0.5 Pa, and then in order to trigger the reduction reaction, aluminum was heated at 800°C while TiO₂ was heated at 300–500°C for 6 h [32]. As shown in Figure 8(b), black TiO₂ nanoparticles can be produced on a large scale with aluminum reduction method. A unique crystalline/amorphous core-shell structure was observed on all Al-reduced TiO₂ prepared at different temperatures, and the thickness of the disordered outer layer increased with the Al-reduction temperature (Figures 8(c), 8(d), 8(e), and 8(f))

[32]. The black TiO₂ absorbed ~65% of the total solar energy by improving visible and infrared absorption and thus exhibited markedly high photoactivity in both photocatalytic water splitting and degradation, superior to the pristine TiO₂ (~5% solar energy absorption) [32].

4.3.2. CaH₂ Reduction. Reduction of TiO₂ (rutile in [83, 84]) by CaH₂ usually generates black Ti₂O₃ rather than black TiO₂ [83, 84]. Recently, black TiO₂ was prepared from Degussa P25 by CaH₂ reduction at 400°C [42]. The black TiO₂ had a crystalline/amorphous core/shell structure with abundant oxygen vacancies, which led to a high solar absorption (~81% solar energy absorption) and significantly enhanced photocatalytic organic degradation and water-splitting performance [42].

4.3.3. Magnesium Reduction. Recently, Sinhamahapatra et al. developed a new method to synthesize black TiO₂ with magnesium as the reductant [11]. Typically, well-mixed reactant of commercial TiO₂ and magnesium powder was placed in a tube furnace and then heated at 650°C for 5 h in the flow of 5% H₂/Ar; the product was stirred for 24 h in 1.0 M HCl

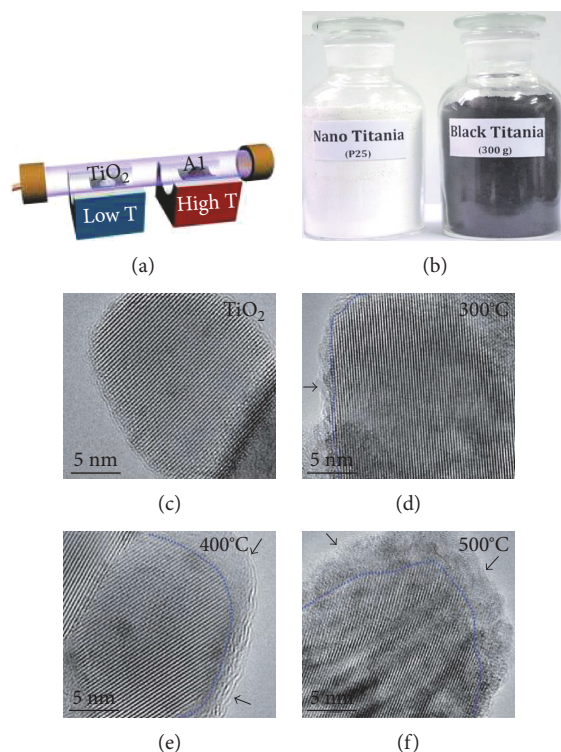


FIGURE 8: (a) Schematic low-temperature reduction of TiO_2 in a two-zone furnace. (b) Digital images of white and black TiO_2 . (c–f) HRTEM images of TiO_2 nanocrystals before (c) and after (d–f) the Al reduction at different temperatures for 6 h. Reprinted with permission from [32]. Copyright (2013) The Royal Society of Chemistry.

and then washed with sufficient amount of water to remove the acid and dried at 80°C [11]. A small amount of anatase was transformed into rutile during the reduction process [11]. The maximum hydrogen production rates were $43\text{ mmol}\cdot\text{h}^{-1}\text{ g}^{-1}$ and $440\text{ }\mu\text{mol}\cdot\text{h}^{-1}\text{ g}^{-1}$, along with remarkable stability under full solar wavelength light and visible light irradiation, respectively [11]. This outstanding activity can be correlated with the extended absorption in visible light, perfect band position, the presence of an appropriate amount of Ti^{3+} species and oxygen vacancies, and slower charge recombination [11].

4.3.4. NaBH_4 Reduction. 3D mesoporous black $\text{TiO}_2/\text{MoS}_2/\text{TiO}_2$ (MBT/ MoS_2 /MBT) nanosheets were prepared by ball milling and subsequent NaBH_4 reduction at 350°C for 1 h under an Ar atmosphere as shown schematically in Figure 9 [85]. The introduction of the TiO_2 - MoS_2 heterojunction and the Ti^{3+} species narrowed the band gap of TiO_2 , leading to the excellent activity in photocatalytic degradation of methyl orange and water splitting for H_2 evolution under visible-light irradiation [85]. The H_2 production rates were 0, 0.13, 0.32, and $0.56\text{ mmol}\cdot\text{h}^{-1}\text{ g}^{-1}$ for mesoporous TiO_2 (MT), mesoporous black TiO_2 (MBT), (MT/ MoS_2 /MT), and (MBT/ MoS_2 /MBT), respectively [85].

4.3.5. Lithium Reduction. Zhang et al. reported that black rutile TiO_2 can be achieved by soaking rutile TiO_2 nanomaterials in a Li-containing ethanediamine solution [86, 87]. Typically, 14 mg of metallic Li foils were dissolved in 20 mL

of ethanediamine under dry conditions; then, 200 mg of TiO_2 nanocrystals (Degussa P25) was immersed into the ethanediamine solution for 6 h with continuous stirring; 1 M HCl was used to consume the excess Li or electrons when the reaction was complete; finally, the product was rinsed with deionized water several times and dried in vacuum oven at room temperature [86]. Note that the Li-assisted reduction is phase selective: rutile phase is reduced into black TiO_2 while anatase phase is well-maintained [86]. This offers us an opportunity to create abundant order/disorder junctions at the surface by controlling the phase composition in pristine TiO_2 for highly efficient photocatalytic hydrogen generation [86]. The order/disorder/water junction was believed to efficiently internally drive the electron/hole separation through type-II bandgap alignment and to trigger a strong hydrogen evolution surface reaction [86]. Furthermore, Zhang et al. found that the “crystal-deficient” layers on the surface of the rutile TiO_2 nanowires increased the conductivity by 50 times, which increased the electron diffusion length to $\sim 20\text{ }\mu\text{m}$ and overcame the charge collection limitation at the solid/liquid interface for efficient conversion of solar energy to chemical energy [87]. These studies highlight the importance of controlling the surface localization of defects and the solid/liquid interface towards enhanced photoactivity over TiO_2 photocatalysts [86–88].

4.4. Black TiO_2 Nanomaterials by Chemical Oxidation. Xin et al. prepared black anatase TiO_2 with a crystalline/amorphous core/shell structure by chemical oxidation method

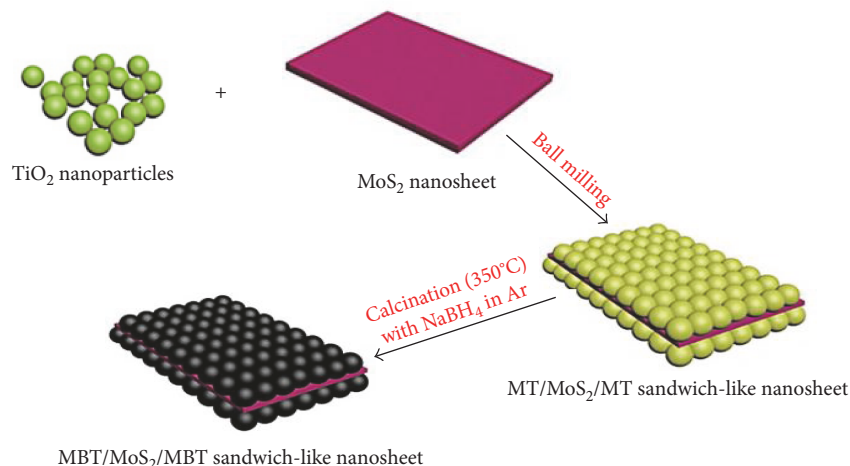


FIGURE 9: Preparation of MBT/MoS₂/MBT sandwich-like nanosheets. Reprinted with permission from [85]. Copyright (2016) Wiley-VCH.

[30]. Typically, a yellowish gel was first obtained by reacting TiH₂ and H₂O₂ for 12 h; then, the gel was diluted using ethanol, the pH of the mixture was adjusted to 9.0 by NaOH, and NaBH₄ as an antioxidant was added to the resulting mixture; after the solvothermal treatment at 180°C for 24 h, the collected sample was washed with HCl, water, and ethanol; light blue TiO₂ nanocrystals (TiO_{2-x}) were obtained after the precipitate was dried in vacuum for 12 h; finally, postannealing treatment was carried out at 300–700°C for 3 h under a nitrogen flow [30]. The annealing temperature was found to be a crucial factor affecting the color of the as-prepared TiO₂ nanocrystals [30]. Light brown, brown, black, dark brown, and shallow dark brown TiO₂ nanocrystals were obtained at 300, 400, 500, 600, and 700°C, respectively [30]. It is found that the Ti³⁺ species initially increased with annealing temperature up to 500°C and then decreased with further temperature rise [30]. The black TiO_{2-x} prepared at 500°C had the highest Ti³⁺ concentration and thus exhibited the highest photocatalytic activity [30].

Similarly, Grabstanowicz et al. reported on black rutile TiO₂ that was prepared by oxidizing TiH₂ in H₂O₂, followed by calcinations in Ar gas [59]. The Ti³⁺ concentration reached as high as one Ti³⁺ per ~4300 Ti⁴⁺ in the black rutile TiO₂, and thus, it exhibited remarkably enhanced visible-light photocatalytic degradation on organic pollutants in water [59]. Xin et al. fabricated black brookite TiO₂ single-crystalline nanosheets by hydrothermal reaction with TiH₂ and H₂O₂ as the Ti source and oxidant, respectively, followed by postannealing treatment at 500°C (T500 in Figure 10(a)) [89]. The black TiO₂ showed drastically enhanced visible-light absorption with a significantly narrowed bandgap of 2.10 eV (Figure 10(a)) owing to the introduction of bulk Ti³⁺ defects [89]. When used as photocatalysts, the black TiO₂ exhibited the highest CO₂ reduction rate (11.9 μmol·g⁻¹·h⁻¹ for CH₄ and 23.5 μmol·g⁻¹·h⁻¹ for CO) (Figure 10(b)) [89].

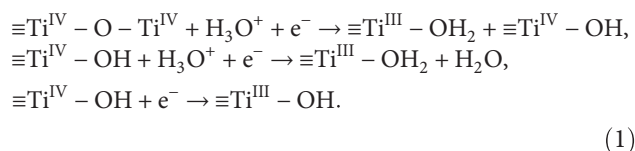
4.5. Black TiO₂ Nanomaterials by Electrochemical Reduction.

The electrochemically reduced black TiO₂ often possessed abundant Ti³⁺ species and oxygen vacancies [17, 56, 90, 91].

The reported black TiO₂ nanomaterials with a nanotube morphology and an anatase phase are prepared by electrochemical reduction in ethylene glycol electrolytes [56, 90, 91]. However, it should be noted that electrochemically reduced black TiO₂ in ethylene glycol electrolytes was not stable [56, 91], because glycerol has a higher viscosity making it difficult for the protons to insert into TiO₂ [91]. It is worth noting that the electrochemically reduced black TiO₂ nanotubes were recently found unstable in air [17].

Xu et al. reported on the electrochemically hydrogenated black TiO₂ nanotubes [90]. The pristine anodic TiO₂ nanotubes were prepared at 150 V for 1 h in an ethylene glycol electrolyte containing 0.3 wt.% NH₄F and 10 vol.% H₂O with carbon rod and Ti foil as the cathode and anode, respectively [90]. After the pristine TiO₂ nanotubes were annealed in air at 150°C for 3 h and then 450°C for 5 h, the electrochemical reduction was performed at 5 V for 5 to 40 s in 0.5 M Na₂SO₄ aqueous solution at room temperature with the TiO₂ nanotubes as the cathode and Pt as the anode to achieve black TiO₂ nanotubes [90]. The surface oxygen vacancies were considered to contribute to the substantially enhanced electrical conductivity and photoactivity [90].

Similarly, Li et al. synthesized black anatase TiO₂ nanotubes by electrochemical reduction [91]. In their study, a so-called “activation” step was adopted in order to obtain stable black TiO₂ nanotubes, where anodization was carried out in an ethylene glycol solution of 0.2 M HF and 0.12 M H₂O₂ at 60 V for 30 s before the electrochemical reduction synthesis of black TiO₂ nanotubes at a cathodic voltage of -40 V for 680 s in an ethylene glycol solution of 0.27 wt.% NH₄F [91]. The authors proposed the doping mechanism as follows:



H⁺ ions were likely driven inside the TiO₂ under the cathodic field [91]. As shown in Figure 11, black TiO₂

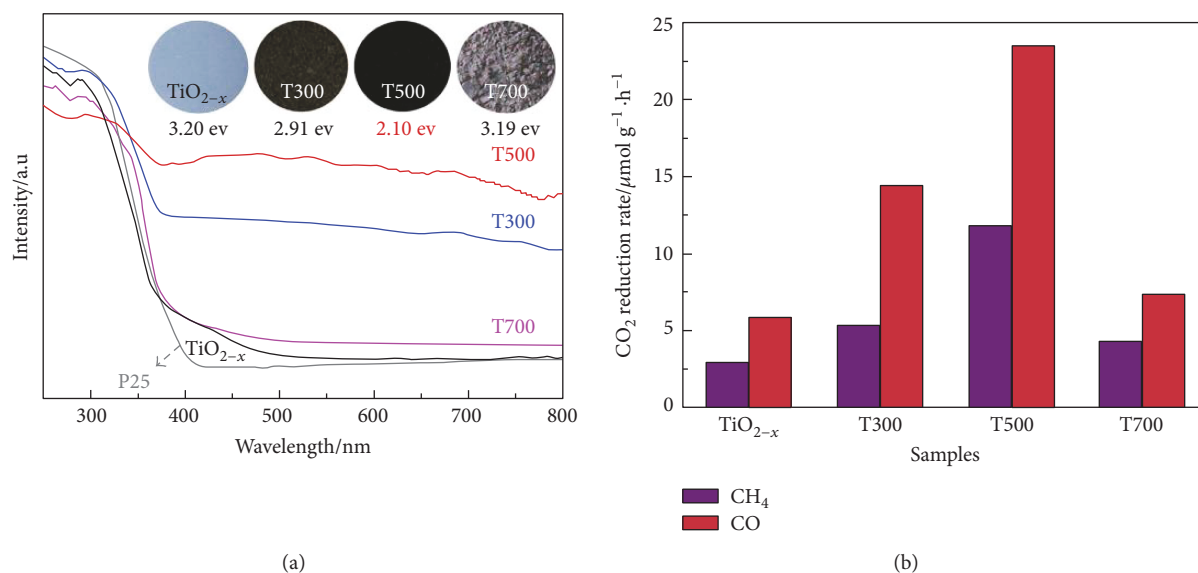


FIGURE 10: (a) UV-vis diffuse reflectance spectra and (b) CO_2 reduction rate of the TiO_{2-x} , T300, T500, and T700. TiO_{2-x} is the as-prepared TiO_2 by hydrothermal reaction. T300, T500, and T700 are the products after postannealing treatment at 300, 500, and 700°C, respectively. Reprinted with permission from [89]. Copyright (2016) Nature Publishing Group.

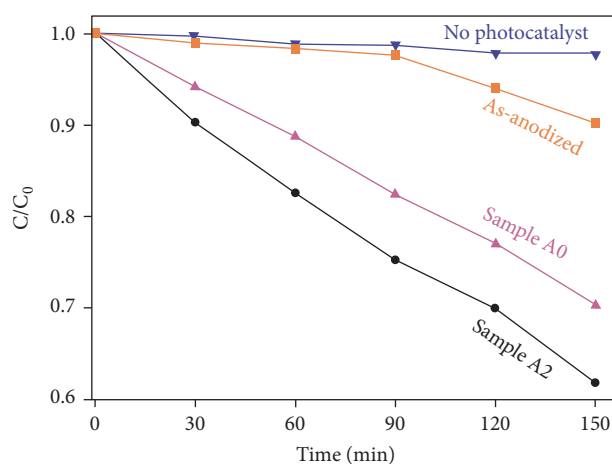


FIGURE 11: Ratio of the actual and initial concentrations (C/C_0) of rhodamine B as a function of the UV illumination time for the as-anodized sample (anodized at 80 V for 7200 s), sample A0 (anodized at 80 V for 7200 s, following by annealing at 450°C for 4 h), and sample A2 (black TiO_2 nanotubes converted from sample A0 via the activation step and subsequent cathodic treatment). The blank experiment was carried out in the absence of any photocatalyst (“no photocatalyst”). Reprinted with permission from [91]. Copyright (2014) The Royal Society of Chemistry.

nanotubes demonstrated the highest photocatalytic activity in rhodamine B degradation experiment, though the as-anodized TiO_2 nanotubes were rich in oxygen vacancies [91].

4.6. Black TiO_2 Nanomaterials by Other Methods

4.6.1. Water-Plasma-Assisted Synthesis. Panomsuwan et al. reported on the water-plasma-assisted synthesis of black titania spheres (H-TiO_{2-x}) with efficient visible-light photocatalytic activity [44]. The H-TiO_{2-x} was composed of a mixture of rutile, anatase, and oxygen-deficient phases (e.g., $\text{Ti}_{10}\text{O}_{19}$,

Ti_5O_9 , and Ti_3O_5). The abundant oxygen vacancies and Ti^{3+} species with the presence of Ti^{2+} species resulted in a narrowed bandgap of 2.18 eV [44]. Under visible-light irradiation for 180 min, the methylene blue is almost completely degraded in the presence of H-TiO_{2-x} (90%), whereas it is degraded only by 18% in the presence of P25 [44].

4.6.2. Nitrogen Doping. Wei’s group focused on the synthesis of crystalline/disordered core-shell black anatase TiO_2 ($\text{TiO}_2@/\text{TiO}_{2-x}$) by a one-step calcination in N_2 [43, 92]. Typically, two mixture solutions were prepared: one containing tetrabutyl titanate, urea, and ethanol absolute and another containing hydrochloric acid, deionized water, and ethanol absolute; the latter was added dropwise to the former solution and stirred until white colloid was formed; the mixture was placed in a water bath at 35°C for 30 min and then stirred magnetically for 2 h; the $\text{TiO}_2@/\text{TiO}_{2-x}$ was obtained by annealing at 550°C for 3 h in a nitrogen atmosphere [43]. Oxygen vacancies and nitrogen species were detected in $\text{TiO}_2@/\text{TiO}_{2-x}$ which explained its narrowed bandgap and high visible light photocatalytic degradation performance on methyl orange [43]. The authors also investigated the effect of urea concentration on the structure and photocatalytic activity of the black TiO_2 and found that a lower urea concentration triggered the largest amount of oxygen vacancies [43].

4.6.3. Electrochemical Oxidation. Defective black anatase TiO_2 nanotubes were synthesized via two-step anodization on Ti foil in ethylene glycol containing 0.25 wt.% NH_4F and 2 vol.% distilled water at 60 V for 10 h, followed by calcination in the air (Figure 12) [54]. The black TiO_2 with controllable level of defects exhibited a high photocatalytic activity under visible light [54]. Mechanistic analysis and characterization results indicated that oxygen vacancies were formed in an oxygen-deficient environment during the anodization

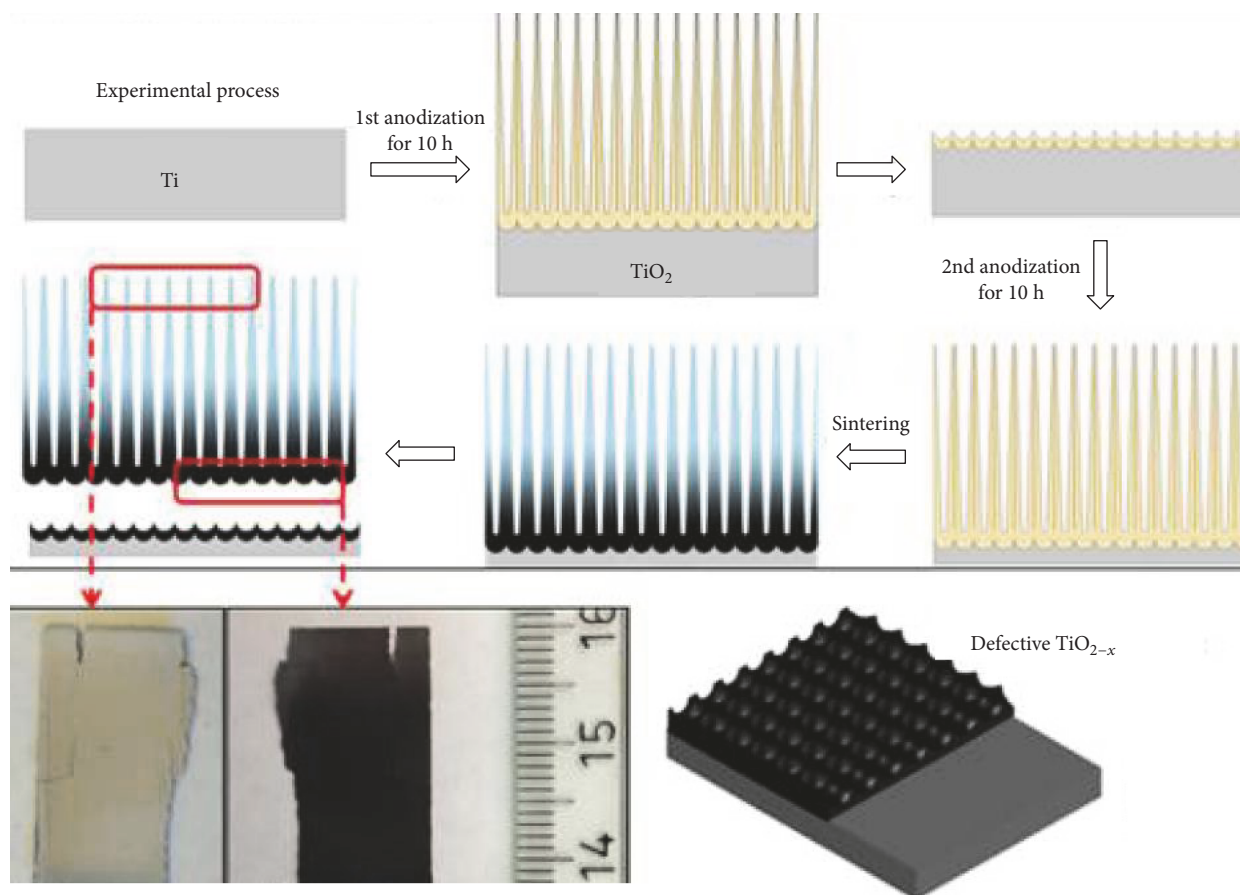


FIGURE 12: Experimental process and optical images of the stripped TiO_2 layer. Reprinted with permission from [54]. Copyright (2014) American Chemical Society.

process and accounted for the high photon-absorbance of the black TiO_2 throughout the visible-light region [54].

4.6.4. Ionothermal Synthesis. Black Ti^{3+} -doped anatase TiO_2 was synthesized by treating metal Ti in an N-N-dimethylformamide solution containing 1-methyl-imidazolium tetrafluoroborate (ionic liquid), lithium acetate, and acetic acid in an autoclave at 200°C for 24 h [55]. The ionic liquid enriched with fluorine and acetic acid play key roles in dissolving and oxidizing the Ti foil, respectively [55]. The in situ generated H_2 from the reaction between Ti foil and acetic acid could be strongly adsorbed onto the surface of TiO_2 and dissociated into H atom to form H-TiO_{2-x} disordered layer [55]. The Ti^{3+} -rich black TiO_2 exhibited high activity in photocatalytic degradation of organic pollutants under visible light ($\lambda > 420 \text{ nm}$) and also a high hydrogen evolution rate of $0.26 \text{ mmol}\cdot\text{h}^{-1}\text{m}^{-2}$ in water splitting under simulated solar light [55].

4.6.5. Laser Irradiation. Black TiO_2 nanospheres were fabricated by laser irradiation on suspended solution containing 20 mg anatase TiO_2 nanospheres and 1 mL distilled water [93]. Phase transformation from anatase to rutile was observed when laser irradiation was performed more than 15 min, and black TiO_2 was obtained after 120 min laser irradiation [93]. The degradation ratio of rhodamine B with

black TiO_2 nanospheres could reach up to 33% under green light for 5 h, while the pristine and P25 showed no degradation ability on rhodamine B [93]. The high photoactivity was attributed to the Ti^{3+} defects and disordered surface layer which resulted in a narrowed bandgap of 2.2 eV [93]. Recently, black amorphous TiO_2 film was achieved by pulsed laser deposition at 100°C for 10 min under vacuum condition using a commercial TiO_2 target and a KrF excimer laser at a repetition rate of 2 Hz with a laser fluence of $2 \text{ J}\cdot\text{cm}^{-2}$ [94]. This black amorphous TiO_2 film was deposited on a pre-deposited crystalline TiO_2 film to construct a bilayer structure similar to the crystalline/amorphous core/shell structure of black TiO_2 nanoparticles in order to create a simpler model to elucidate the working mechanism of black TiO_2 nanomaterials in many applications [94]. Metallic conduction was achieved at the crystalline/amorphous homointerface via electronic interface reconstruction [94]. This points to a research direction that may partly elucidate the high performance of black TiO_2 in many applications.

4.6.6. Proton Implantation. Liu's group applied proton implantation method to the synthesis of black TiO_2 nanotubes [95]. Proton implantation was carried out at an energy of 30 keV and a nominal dose of $10^{16} \text{ ions}\cdot\text{cm}^{-2}$ using a Varian 350 D ion implanter [95]. While the ion implantation on a (001) surface plane of an anatase crystal led to a low H_2

production efficiency, implantation of TiO₂ nanotubes markedly enhanced hydrogen evolution due to the length effect [95]. That is, a synergistic interaction between the implanted upper part of the TiO₂ nanotube, acting as light absorber, and the intact lower part, acting as catalytically active center, was proposed [95].

5. Summary and Prospective

TiO₂ photocatalyst as an ideal model for the investigation of photocatalysis in a variety of areas has attracted enormous attention over the past decades, especially on the water splitting for hydrogen production, pollutant removal for environmental protection and CO₂ reduction for solar fuels. These aspects are significant to the sustainable development of the economy and human society. However, the solar energy conversion efficiency is quite low owing to the limited optical absorption of TiO₂ only to UV spectrum and the rapid electron-hole recombination. Structural engineering that mainly leads to surface structure change of TiO₂ with color change from whiteness to blackness is a promising strategy. This strategy has the potential to take care of both sides, that is, black TiO₂ nanomaterials often exhibit a large absorption of visible light and highly enhanced charge separation. Many synthetic approaches have been developed to synthesize surface-structure-engineered black TiO₂ nanomaterials since the report of the hydrogenated black TiO₂ crystals in 2011. Despite these progress, two main challenges are present in terms of synthesis and applications of black TiO₂. (i) Optical absorption of visible light, at present, does not mean their successful conversion to solar fuels; increasing the effective utilization of visible light is still a challenge for black TiO₂. (ii) Scalable synthesis of black TiO₂ with highly controllable quality is of vital importance for its practical applications. On the other hand, there are still quite a few open questions: why black TiO₂ nanomaterials have much higher photocatalytic activity over normal white TiO₂ nanomaterials (however, note that not all black TiO₂ nanomaterials exhibited enhanced photoactivity); what on earth primarily triggers the optical absorption of black TiO₂ nanomaterials to visible light; what are the individual roles of different types of defects in black TiO₂ nanomaterials; how the defect-rich surface region in black TiO₂ nanomaterials affects the charge transfer and photoactivity; etc. The answers to these fundamental questions vary with preparation method, properties of pristine TiO₂, et al. This may be owing to the high sensitivity of the optical and electronic properties of TiO₂ to its surface structure. The huge differences in the surface structures (including surface groups, types and quantities of defects, and heteroatom contamination) among different black TiO₂ make the fundamental understanding even harder. Therefore, novel strategies along with new technologies that can precisely control and probe the surface structural evolution during the preparation process are highly desired. TiO₂ with quantitatively controlled surface defects may be a good model to reveal the underlying working principle of black TiO₂ nanomaterials in photocatalysis. The interface between the crystalline core and the disordered surface layer may also be an important consideration for understanding the basic

physicochemical properties of black TiO₂, but less attention has been paid to that. On the other hand, the interaction between the reactant compounds/ions and the surface of black TiO₂ nanomaterials, especially the effects of their surface states on the adsorption and activation of the targeted reactants, also calls for more attention as different photocatalytic processes need slightly different reaction environments which are highly related to the surface structures. We hope this review can inspire more work to advance the understanding and development of the black TiO₂ in photocatalysis.

Conflicts of Interest

The authors declare that they have no conflict of interest.

Acknowledgments

Xiaodong Yan thanks the funds provided by the University of Missouri-Kansas City, School of Graduate Studies.

References

- [1] A. Fujishima and K. Honda, "Electrochemical photolysis of water at a semiconductor electrode," *Nature*, vol. 238, no. 5358, pp. 37-38, 1972.
- [2] X. Yan and X. Chen, "Titanium dioxide nanomaterials," in *Encyclopedia of Inorganic and Bioinorganic Chemistry*, pp. 1-38, John Wiley & Sons, 2015.
- [3] X. Chen and S. S. Mao, "Titanium dioxide nanomaterials: synthesis, properties, modifications, and applications," *Chemical Reviews*, vol. 107, no. 7, pp. 2891-2959, 2007.
- [4] Y.-H. Lin, C.-H. Weng, J.-H. Tzeng, and Y.-T. Lin, "Adsorption and photocatalytic kinetics of visible-light response N-doped TiO₂ nanocatalyst for indoor acetaldehyde removal under dark and light conditions," *International Journal of Photoenergy*, vol. 2016, Article ID 3058429, 9 pages, 2016.
- [5] P. Yao, S. Zhong, and Z. Shen, "TiO₂/halloysite composites codoped with carbon and nitrogen from melamine and their enhanced solar-light-driven photocatalytic performance," *International Journal of Photoenergy*, vol. 2015, Article ID 605690, 8 pages, 2015.
- [6] T. Xia, Y. Zhang, J. Murowchick, and X. Chen, "Vacuum-treated titanium dioxide nanocrystals: optical properties, surface disorder, oxygen vacancy, and photocatalytic activities," *Catalysis Today*, vol. 225, pp. 2-9, 2014.
- [7] H. G. Yang, C. H. Sun, S. Z. Qiao et al., "Anatase TiO₂ single crystals with a large percentage of reactive facets," *Nature*, vol. 453, no. 7195, pp. 638-641, 2008.
- [8] F. Liu, X. Yan, X. Chen, L. Tian, Q. Xia, and X. Chen, "Mesoporous TiO₂ nanoparticles terminated with carbonate-like groups: amorphous/crystalline structure and visible-light photocatalytic activity," *Catalysis Today*, vol. 264, pp. 243-249, 2016.
- [9] H. Wang, T. Lin, G. Zhu et al., "Colored titania nanocrystals and excellent photocatalysis for water cleaning," *Catalysis Communications*, vol. 60, pp. 55-59, 2015.
- [10] S. N. Habisreutinger, L. Schmidt-Mende, and J. K. Stolarczyk, "Photocatalytic reduction of CO₂ on TiO₂ and other semiconductors," *Angewandte Chemie International Edition*, vol. 52, pp. 7372-7408, 2013.

- [11] A. Sinhamahapatra, J. P. Jeon, and Y. JS, "A new approach to prepare highly active and stable black titania for visible light-assisted hydrogen production," *Energy & Environmental Science*, vol. 8, pp. 3539–3544, 2015.
- [12] V. A. Lebedev, D. A. Kozlov, I. V. Kolesnik et al., "The amorphous phase in titania and its influence on photocatalytic properties," *Applied Catalysis B: Environmental*, vol. 195, pp. 39–47, 2016.
- [13] L. G. Bettini, M. V. Dozzi, F. D. Foglia et al., "Mixed-phase nanocrystalline TiO₂ photocatalysts produced by flame spray pyrolysis," *Applied Catalysis B: Environmental*, vol. 178, pp. 226–232, 2015.
- [14] F. Zuo, L. Wang, T. Wu, Z. Zhang, D. Borchardt, and P. Feng, "Self-doped Ti³⁺ enhanced photocatalyst for hydrogen production under visible light," *Journal of the American Chemical Society*, vol. 132, no. 34, pp. 11856–11857, 2010.
- [15] X. Pan, M. Q. Yang, X. Fu, N. Zhang, and Y. J. Xu, "Defective TiO₂ with oxygen vacancies: synthesis, properties and photocatalytic applications," *Nanoscale*, vol. 5, no. 9, pp. 3601–3614, 2013.
- [16] S. T. Myung, M. Kikuchi, C. S. Yoon et al., "Black anatase titania enabling ultra high cycling rates for rechargeable lithium batteries," *Energy & Environmental Science*, vol. 6, pp. 2609–2614, 2013.
- [17] N. Liu, C. Schneider, D. Freitag, E. M. Zolnhofer, K. Meyer, and P. Schmuki, "Noble-metal-free photocatalytic H₂ generation: active and inactive 'black' TiO₂ nanotubes and synergistic effects," *Chemistry - A European Journal*, vol. 22, no. 39, pp. 13810–13814, 2016.
- [18] L. Jing, W. Zhou, G. Tian, and H. Fu, "Surface tuning for oxide-based nanomaterials as efficient photocatalysts," *Chemical Society Reviews*, vol. 42, no. 24, pp. 9509–9549, 2013.
- [19] R. Asahi, T. Morikawa, T. Ohwaki, K. Aoki, and Y. Taga, "Visible-light photocatalysis in nitrogen-doped titanium oxides," *Science*, vol. 293, no. 5528, pp. 269–271, 2001.
- [20] S. Linic, P. Christopher, and D. B. Ingram, "Plasmonic-metal nanostructures for efficient conversion of solar to chemical energy," *Nature Materials*, vol. 10, no. 12, pp. 911–921, 2011.
- [21] E. Kowalska, R. Abe, and B. Ohtani, "Visible light-induced photocatalytic reaction of gold-modified titanium(IV) oxide particles: action spectrum analysis," *Chemical Communications*, no. 2, pp. 241–243, 2009.
- [22] X. Chen, L. Liu, P. Y. Yu, and S. S. Mao, "Increasing solar absorption for photocatalysis with black hydrogenated titanium dioxide nanocrystals," *Science*, vol. 331, no. 6018, pp. 746–750, 2011.
- [23] A. Naldoni, M. Allieta, S. Santangelo et al., "Effect of nature and location of defects on bandgap narrowing in black TiO₂ nanoparticles," *Journal of the American Chemical Society*, vol. 134, no. 18, pp. 7600–7603, 2012.
- [24] D. A. H. Hanaor and C. C. Sorrell, "Review of the anatase to rutile phase transformation," *Journal of Materials Science*, vol. 46, pp. 855–874, 2011.
- [25] Y. Ma, X. Wang, Y. Jia, X. Chen, H. Han, and C. Li, "Titanium dioxide-based nanomaterials for photocatalytic fuel generations," *Chemical Reviews*, vol. 114, no. 19, pp. 9987–10043, 2014.
- [26] S. Liu, H. Jia, L. Han et al., "Nanosheet-constructed porous TiO₂-B for advanced lithium ion batteries," *Advanced Materials*, vol. 24, no. 24, pp. 3201–3204, 2012.
- [27] T. A. Kaniel, L. Robben, and A. Alkaim, "Brookite versus anatase TiO₂ photocatalysts: phase transformations and photocatalytic activities," *Photochemical & Photobiological Sciences*, vol. 12, no. 4, pp. 602–609, 2013.
- [28] H. Zhang and J. F. Banfield, "Understanding polymorphic phase transformation behavior during growth of nanocrystalline aggregates: insights from TiO₂," *The Journal of Physical Chemistry B*, vol. 104, pp. 3481–3487, 2000.
- [29] M. Salari, K. Konstantinov, and H. K. Liu, "Enhancement of the capacitance in TiO₂ nanotubes through controlled introduction of oxygen vacancies," *Journal of Materials Chemistry*, vol. 21, pp. 5128–5133, 2011.
- [30] X. Xin, T. Xu, J. Yin, L. Wang, and C. Wang, "Management on the location and concentration of Ti³⁺ in anatase TiO₂ for defects-induced visible-light photocatalysis," *Applied Catalysis B: Environmental*, vol. 176, pp. 354–362, 2015.
- [31] T. Xia and X. Chen, "Revealing the structural properties of hydrogenated black TiO₂ nanocrystals," *Journal of Materials Chemistry A*, vol. 1, pp. 2983–2989, 2013.
- [32] Z. Wang, C. Yang, T. Lin et al., "Visible-light photocatalytic, solar thermal and photoelectrochemical properties of aluminium-reduced black titania," *Energy & Environmental Science*, vol. 6, pp. 3007–3014, 2013.
- [33] Z. Wang, C. Yang, T. Lin et al., "H-doped black titania with very high solar absorption and excellent photocatalysis enhanced by localized surface plasmon resonance," *Advanced Functional Materials*, vol. 23, pp. 5444–5450, 2013.
- [34] X. Chen, L. Liu, Z. Liu et al., "Properties of disorder-engineered black titanium dioxide nanoparticles through hydrogenation," *Scientific Reports*, vol. 3, p. 1510, 2013.
- [35] L. Liu, P. Y. Yu, X. Chen, S. S. Mao, and D. Z. Shen, "Hydrogenation and disorder in engineered black TiO₂," *Physical Review Letters*, vol. 111, no. 6, article 065505, 2013.
- [36] H. Lu, B. Zhao, R. Pan et al., "Safe and facile hydrogenation of commercial Degussa P25 at room temperature with enhanced photocatalytic activity," *RSC Advances*, vol. 4, pp. 1128–1132, 2014.
- [37] C. Yang, Z. Wang, T. Lin et al., "Core-shell nanostructured 'black' rutile titania as excellent catalyst for hydrogen production enhanced by sulfur doping," *Journal of the American Chemical Society*, vol. 135, no. 47, pp. 17831–17838, 2013.
- [38] T. Lin, C. Yang, Z. Wang et al., "Effective nonmetal incorporation in black titania with enhanced solar energy utilization," *Energy & Environmental Science*, vol. 7, pp. 967–972, 2013.
- [39] F. Teng, M. Li, C. Gao et al., "Preparation of black TiO₂ by hydrogen plasma assisted chemical vapor deposition and its photocatalytic activity," *Applied Catalysis B: Environmental*, vol. 148–149, pp. 339–343, 2014.
- [40] Y. Zhu, D. Liu, and M. Meng, "H₂ spillover enhanced hydrogenation capability of TiO₂ used for photocatalytic splitting of water: a traditional phenomenon for new applications," *Chemical Communications*, vol. 50, pp. 6049–6051, 2014.
- [41] G. Zhu, T. Lin, X. Lü et al., "Black brookite titania with high solar absorption and excellent photocatalytic performance," *Journal of Materials Chemistry A*, vol. 1, pp. 9650–9653, 2013.
- [42] G. Zhu, H. Yin, C. Yang et al., "Black titania for superior photocatalytic hydrogen production and photoelectrochemical water splitting," *ChemCatChem*, vol. 7, pp. 2614–2619, 2015.

- [43] S. Wei, R. Wu, X. Xu, J. Jian, H. Wang, and Y. Sun, "One-step synthetic approach for core-shelled black anatase titania with high visible light photocatalytic performance," *Chemical Engineering Journal*, vol. 229, pp. 120–125, 2016.
- [44] G. Panomsuwan, A. Watthanaphanit, T. Ishizaki, and N. Saito, "Water-plasma-assisted synthesis of black titania spheres with efficient visible-light photocatalytic activity," *Physical Chemistry Chemical Physics*, vol. 17, no. 21, pp. 13794–13799, 2015.
- [45] G. Wang, H. Wang, Y. Ling et al., "Hydrogen-treated TiO₂ nanowire arrays for photoelectrochemical water splitting," *Nano Letters*, vol. 11, no. 7, pp. 3026–3033, 2011.
- [46] Z. Lu, C. T. Yip, L. Wang, H. Huang, and L. Zhou, "Hydrogenated TiO₂ nanotube arrays as high-rate anodes for lithium-ion microbatteries," *ChemPlusChem*, vol. 77, pp. 991–1000, 2012.
- [47] Z. Zheng, B. Huang, J. Lu et al., "Hydrogenated titania: synergy of surface modification and morphology improvement for enhanced photocatalytic activity," *Chemical Communications*, vol. 48, pp. 5733–5735, 2012.
- [48] M. V. Ganduglia-Pirovano, A. Hofmann, and J. Sauer, "Oxygen vacancies in transition metal and rare earth oxides: current state of understanding and remaining challenges," *Surface Science Reports*, vol. 62, pp. 219–270, 2007.
- [49] G. Pacchioni, "Oxygen vacancy: the invisible agent on oxide surfaces," *ChemPhysChem*, vol. 4, no. 10, pp. 1041–1047, 2003.
- [50] N. G. Petrik and G. A. Kimmel, "Reaction kinetics of water molecules with oxygen vacancies on rutile TiO₂(110)," *The Journal of Physical Chemistry C*, vol. 119, pp. 23059–23067, 2015.
- [51] R. Schaub, P. Thstrup, N. Lopez et al., "Oxygen vacancies as active sites for water dissociation on rutile TiO₂(110)," *Physical Review Letters*, vol. 87, no. 26, article 266104, 2001.
- [52] N. Liu, C. Schneider, D. Freitag et al., "Black TiO₂ nanotubes: cocatalyst-free open-circuit hydrogen generation," *Nano Letters*, vol. 14, no. 6, pp. 3309–3313, 2014.
- [53] H. Cui, W. Zhao, C. Yang et al., "Black TiO₂ nanotube arrays for high-efficiency photoelectrochemical water-splitting," *Journal of Materials Chemistry A*, vol. 2, pp. 8612–8616, 2014.
- [54] J. Dong, J. Han, Y. Liu et al., "Defective black TiO₂ synthesized via anodization for visible-light photocatalysis," *ACS Applied Materials & Interfaces*, vol. 6, no. 3, pp. 1385–1388, 2014.
- [55] G. Li, Z. Lian, X. Li et al., "Ionothermal synthesis of black Ti³⁺-doped single-crystal TiO₂ as an active photocatalyst for pollutant degradation and H₂ generation," *Journal of Materials Chemistry A*, vol. 3, pp. 3748–3756, 2015.
- [56] H. Zhou and Y. Zhang, "Electrochemically self-doped TiO₂ nanotube arrays for supercapacitors," *The Journal of Physical Chemistry C*, vol. 118, no. 11, pp. 5626–5636, 2014.
- [57] Y. Yan, M. Han, A. Konkin et al., "Slightly hydrogenated TiO₂ with enhanced photocatalytic performance," *Journal of Materials Chemistry A*, vol. 2, pp. 12708–12716, 2014.
- [58] A. Lepcha, C. Maccato, A. Mettenbörger et al., "Electrospun black titania nanofibers: influence of hydrogen plasma-induced disorder on the electronic structure and photoelectrochemical performance," *The Journal of Physical Chemistry C*, vol. 119, pp. 18835–18842, 2015.
- [59] L. R. Grabstanowicz, S. Gao, T. Li et al., "Facile oxidative conversion of TiH₂ to high-concentration Ti³⁺-self-doped rutile TiO₂ with visible-light photoactivity," *Inorganic Chemistry*, vol. 52, no. 7, pp. 3884–3890, 2013.
- [60] W. Ren, Y. Yan, L. Zeng et al., "A near infrared light triggered hydrogenated black TiO₂ for cancer photothermal therapy," *Advanced Healthcare Materials*, vol. 4, pp. 1526–1536, 2015.
- [61] X. Chen and C. Burda, "The electronic origin of the visible-light absorption properties of C-, N- and S-doped TiO₂ nanomaterials," *Journal of the American Chemical Society*, vol. 130, no. 15, pp. 5018–5019, 2008.
- [62] S. U. M. Khan, M. Al-Shahry, and W. B. J. Ingler, "Efficient photochemical water splitting by a chemically modified n-TiO₂," *Science*, vol. 297, no. 5590, pp. 2243–2245, 2002.
- [63] J. Qiu, C. Lai, E. Gray et al., "Blue hydrogenated lithium titanate as a high-rate anode material for lithium-ion batteries," *Journal of Materials Chemistry A*, vol. 2, pp. 6353–6358, 2014.
- [64] W. Choi, A. Termin, and M. R. Hoffmann, "The role of metal ion dopants in quantum-sized TiO₂: correlation between photoreactivity and charge carrier recombination dynamics," *The Journal of Physical Chemistry*, vol. 98, pp. 13669–13679, 1994.
- [65] M. Anpo and M. Takeuchi, "The design and development of highly reactive titanium oxide photocatalysts operating under visible light irradiation," *Journal of Catalysis*, vol. 216, pp. 505–516, 2003.
- [66] U. Diebold, "The surface science of titanium dioxide," *Surface Science Reports*, vol. 48, pp. 53–229, 2003.
- [67] J. Wang, P. Zhang, X. Li, J. Zhu, and H. Li, "Synchronical pollutant degradation and H₂ production on a Ti³⁺-doped TiO₂ visible photocatalyst with dominant (0 0 1) facets," *Applied Catalysis B: Environmental*, vol. 134–135, pp. 198–204, 2013.
- [68] Y. Zhou, C. Chen, N. Wang, Y. Li, and H. Ding, "Stable Ti³⁺ self-doped anatase-rutile mixed TiO₂ with enhanced visible light utilization and durability," *The Journal of Physical Chemistry C*, vol. 120, pp. 6116–6124, 2016.
- [69] I. Nakamura, N. Negishi, S. Kutsuna, T. Ihara, S. Sugihara, and K. Takeuchi, "Role of oxygen vacancy in the plasma-treated TiO₂ photocatalyst with visible light activity for NO removal," *Journal of Molecular Catalysis A: Chemical*, vol. 161, pp. 205–212, 2000.
- [70] L. Jing, B. Xin, F. Yuan, L. Xue, B. Wang, and H. Fu, "Effects of surface oxygen vacancies on photophysical and photochemical processes of Zn-doped TiO₂ nanoparticles and their relationships," *The Journal of Physical Chemistry B*, vol. 110, no. 36, pp. 17860–17865, 2006.
- [71] W. Li, R. Liang, A. Hu, Z. Huang, and Y. Norman Zhou, "Generation of oxygen vacancies in visible light activated one-dimensional iodine TiO₂ photocatalysts," *RSC Advances*, vol. 4, no. 70, pp. 36959–36966, 2014.
- [72] B. Jiang, Y. Tang, Y. Qu et al., "Thin carbon layer coated Ti³⁺-TiO₂ nanocrystallites for visible-light driven photocatalysis," *Nanoscale*, vol. 7, no. 11, pp. 5035–5045, 2015.
- [73] F. Amano, M. Nakata, A. Yamamoto, and T. Tanaka, "Effect of Ti³⁺ ions and conduction band electrons on photocatalytic and photoelectrochemical activity of rutile titania for water oxidation," *The Journal of Physical Chemistry C*, vol. 120, pp. 6467–6474, 2016.
- [74] M. Pelaez, N. T. Nolan, S. C. Pillai et al., "A review on the visible light active titanium dioxide photocatalysts for environmental applications," *Applied Catalysis B: Environmental*, vol. 125, pp. 331–349, 2012.
- [75] J. Y. Shi, J. Chen, Z. C. Feng et al., "Photoluminescence characteristics of TiO₂ and their relationship to the photoassisted

- reaction of water/methanol mixture,” *The Journal of Physical Chemistry C*, vol. 111, pp. 693–699, 2007.
- [76] T. Leshuk, R. Parviz, P. Everett, H. Krishnakumar, R. A. Varin, and F. Gu, “Photocatalytic activity of hydrogenated TiO₂,” *ACS Applied Materials & Interfaces*, vol. 5, no. 6, pp. 1892–1895, 2013.
- [77] J. Y. Eom, S. J. Lim, S. M. Lee, W. H. Ryu, and H. S. Kwon, “Black titanium oxide nanoarray electrodes for high rate Li-ion microbatteries,” *Journal of Materials Chemistry A*, vol. 3, pp. 11183–11188, 2015.
- [78] W. Zhou, W. Li, J. Q. Wang et al., “Ordered mesoporous black TiO₂ as highly efficient hydrogen evolution photocatalyst,” *Journal of the American Chemical Society*, vol. 136, no. 26, pp. 9280–9283, 2014.
- [79] C. Sun, Y. Jia, X. H. Yang et al., “Hydrogen incorporation and storage in well-defined nanocrystals of anatase titanium dioxide,” *The Journal of Physical Chemistry C*, vol. 115, pp. 25590–25594, 2011.
- [80] A. Danon, K. Bhattacharyya, B. K. Vijayan et al., “Effect of reactor materials on the properties of titanium oxide nanotubes,” *ACS Catalysis*, vol. 2, pp. 45–49, 2012.
- [81] Y. He, O. Dulub, H. Cheng, A. Selloni, and U. Diebold, “Evidence for the predominance of subsurface defects on reduced anatase TiO₂(101),” *Physical Review Letters*, vol. 102, no. 10, article 106105, 2009.
- [82] P. Scheiber, M. Fidler, O. Dulub et al., “(Sub)surface mobility of oxygen vacancies at the TiO₂ anatase (101) surface,” *Physical Review Letters*, vol. 109, no. 13, article 136103, 2012.
- [83] S. Tominaka, Y. Tsujimoto, Y. Matsushita, and K. Yamaura, “Synthesis of nanostructured reduced titanium oxide: crystal structure transformation maintaining nanomorphology,” *Angewandte Chemie*, vol. 50, pp. 7418–7421, 2011.
- [84] S. Tominaka, “Topotactic reduction yielding black titanium oxide nanostructures as metallic electronic conductors,” *Inorganic Chemistry*, vol. 51, no. 19, pp. 10136–10140, 2012.
- [85] X. Liu, Z. Xing, H. Zhang et al., “Fabrication of 3D mesoporous black TiO₂/MoS₂/TiO₂ nanosheets for visible-light-driven photocatalysis,” *ChemSusChem*, vol. 9, no. 10, pp. 1118–1124, 2016.
- [86] K. Zhang, L. Wang, J. K. Kim et al., “An order/disorder/water junction system for highly efficient co-catalyst-free photocatalytic hydrogen generation,” *Energy & Environmental Science*, vol. 9, pp. 499–503, 2016.
- [87] K. Zhang, S. Ravishankar, M. Ma et al., “Overcoming charge collection limitation at solid/liquid interface by a controllable crystal deficient overlayer,” *Advanced Energy Materials*, vol. 7, no. 3, article 1600923, 2017.
- [88] K. Zhang and J. H. Park, “Surface localization of defects in black TiO₂: enhancing photoactivity or reactivity,” *The Journal of Physical Chemistry Letters*, vol. 8, no. 1, pp. 199–207, 2017.
- [89] X. Xin, T. Xu, L. Wang, and C. Wang, “Ti³⁺-self doped brookite TiO₂ single-crystalline nanosheets with high solar absorption and excellent photocatalytic CO₂ reduction,” *Scientific Reports*, vol. 6, article 23684, 2016.
- [90] C. Xu, Y. Song, L. Lu et al., “Electrochemically hydrogenated TiO₂ nanotubes with improved photoelectrochemical water splitting performance,” *Nanoscale Research Letters*, vol. 8, no. 1, pp. 391–397, 2013.
- [91] H. Li, Z. Chen, C. K. Tsang et al., “Electrochemical doping of anatase TiO₂ in organic electrolytes for high-performance supercapacitors and photocatalysts,” *Journal of Materials Chemistry A*, vol. 2, pp. 229–236, 2014.
- [92] S. Wei, R. Wu, J. Jian, F. Chen, and Y. Sun, “Black and yellow anatase titania formed by (H, N)-doping: strong visible-light absorption and enhanced visible-light photocatalysis,” *Dalton Transactions*, vol. 44, no. 4, pp. 1534–1538, 2015.
- [93] X. Chen, D. Zhao, K. Liu et al., “Laser-modified black titanium oxide nanospheres and their photocatalytic activities under visible light,” *ACS Applied Materials & Interfaces*, vol. 7, no. 29, pp. 16070–16077, 2015.
- [94] X. Lü, A. Chen, Y. Luo et al., “Conducting interface in oxide homojunction: understanding of superior properties in black TiO₂,” *Nano Letters*, vol. 16, no. 9, pp. 5751–5755, 2016.
- [95] N. Liu, V. Häublein, X. Zhou et al., ““Black” TiO₂ nanotubes formed by high-energy proton implantation show noble-metal-co-catalyst free photocatalytic H₂-evolution,” *Nano Letters*, vol. 15, no. 10, pp. 6815–6820, 2015.

